Nondestructive diagnostic for electron bunch length in accelerators using the wakefield radiation spectrum

S. V. Shchelkunov,[1] T. C. Marshall,[1] J. L. Hirshfield,[2,3] and M. A. LaPointe[2]
[1]*Department of Applied Physics, Columbia University, New York City, New York 10027, USA*
[2]*Department of Physics, Yale University, New Haven, Connecticut 06520-8120, USA*
[3]*Omega-P, Inc., New Haven, Connecticut 06520, USA*
(Received 31 January 2005; published 6 June 2005)

We report the development of a nondestructive technique to measure bunch rms length in the psec range and below, and eventually in the fsec range, by measuring the high-frequency spectrum of wakefield radiation which is caused by the passage of a relativistic electron bunch through a channel surrounded by a dielectric. We demonstrate numerically that the generated spectrum is determined by the rms bunch length, while the specific axial and longitudinal charge distribution is not important. Measurement of the millimeter-wave spectrum will determine the rms bunch length in the psec range. This has been done using a series of calibrated mesh filters and the charge bunches produced by the 50 MeV rf linac system at ATF (Accelerator Test Facility), Brookhaven. We have developed the analysis of the factors crucial for achieving good accuracy in this measurement, and find the experimental data are fully understood by the theory. We point out that this technique also may be used for measuring fsec bunch lengths, using a prepared planar wakefield microstructure.

DOI: 10.1103/PhysRevSTAB.8.062801 PACS numbers: 41.85.Qg, 41.75.Ht, 41.60.Bq, 84.40.−x

I. INTRODUCTION

There are a number of diagnostics which have been used to measure the axial length of relativistic electron bunches in the picosecond (psec) and sub-psec ranges, corresponding to lengths of 1000 μm and less [1]. Among these are coherent transition radiation, diffraction radiation, synchrotron radiation, energy modulation, spontaneous emission single-shot spectrum, and electro-optical detection. Various rf pickup structures (e.g., loop, stripline, resonant cavity) are used to detect the transient radiation produced by the bunch [2]. Certain techniques (e.g., monitoring Cerenkov radiation when the bunch traverses a solid target) can result in destruction of the bunch. Each diagnostic has its advantages and disadvantages. Ideally, one would want a diagnostic that disturbs the bunch as little as possible, and that uses instrumentation that is inexpensive, easy to adjust, and routine to calibrate. In this paper we describe a nondestructive diagnostic which can measure the rms bunch length using an observation of the frequency spectrum of wakefield radiation set up as the bunch passes through a vacuum channel in a hollow dielectric element [3].

Operation of the new diagnostic device is based on the following principles. A bunch or train of bunches enters a short section of beam pipe into which a hollow dielectric liner has been inserted. The dielectric can be made of alumina, which has low losses and good vacuum properties. Inside this structure, the bunch emits coherent Cerenkov radiation, which can be extracted and detected externally. The bunch passes along the axis of the structure and through a vacuum channel in the dielectric; the transverse size of this channel can be chosen to control the interaction and the energy radiated by the bunch. The smaller the width of the channel, the greater is the intensity of the Cerenkov radiation; but the greater also is the drag (or perturbation) on the bunch's motion. The radiation will follow the bunch down the vacuum pipe, and when the radiation is diverted, it can be extracted from the vacuum by passing it through a suitable window. The axisymmetric bunch excites a spectrum of copropagating waveguide modes that constitute a periodic wakefield disturbance following the bunch. Roughly speaking, the power spectrum of these modes is a function that increases with frequency for radiation whose wavelengths exceed the bunch length, decreases with frequency for shorter wavelengths, and falls to negligible amplitude beyond a cutoff frequency. This is a common feature for bunches radiating coherently, where the radiated power scales as N_b^2, with N_b being the number of electrons in the bunch. Thus, mm-size bunches exhibit a transition from a rising power spectrum to a falling power spectrum at a wavelength in the mm range. Interest within the accelerator community in a new bunch-length monitor is ever intensifying for bunches of mm and sub-mm dimensions, so the instrumentation described here is designed to operate in this wavelength region. We also point out that a bunch-length diagnostic for laser accelerators, where the length is in the fsec range, would be useful too.

II. DIAGNOSTIC FOR MM-DIMENSION BUNCHES

In this section, we take the apparatus used to extract diagnostic information from passing charge bunches to be an annular cylinder of low-loss dielectric inserted into a close-fitting metallic drift tube forming part of an evacu-

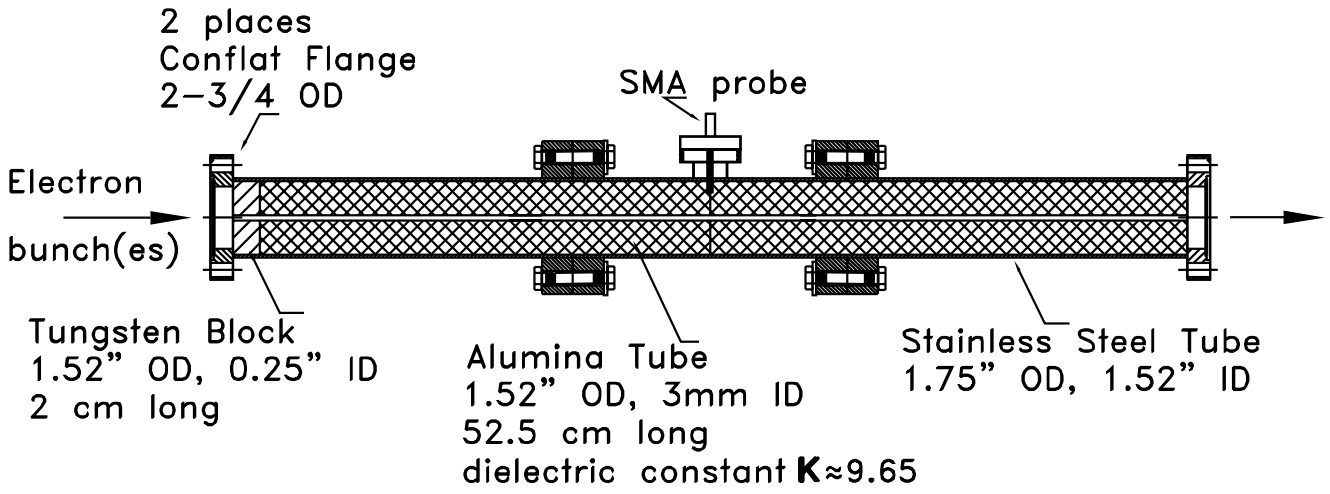

FIG. 1. Diagram of the dielectric-lined beam line element installed in the Omega-P/Yale/Columbia experiment at ATF, Brookhaven for studying wakefields.

ated beam transport line. Our experience with such structures shows that a suitable dielectric in the range of millimeter wavelengths would be alumina [$\kappa \approx 9.6$] which, in addition to having good vacuum properties and low losses, is nearly free of dispersion in the microwave and mm-wave portions of the spectrum [4]. The outer radius of the alumina is $\sim$1.93 cm, and a 3 mm diameter axisymmetric circular cross-section channel allows propagation of the bunch through vacuum. The length of the dielectric section does not play an important role in determining the radiation spectrum, provided the length exceeds a few times the transition radiation zone length near the entrance and exit of the channel [5]. For the dimensions given above, a dielectric length of a few tens of cm is a good choice. This is to insure that Cerenkov wakefield radiation dominates the transition radiation that is emitted as the bunch enters or leaves the structure. Furthermore, experience has shown that charge evidently does not accumulate on the surface of ceramics such as alumina, as it may on other dielectrics.

Figure 1 is a diagram of the dielectric-lined beam line element installed in the Omega-P/Yale/Columbia experiment at ATF (Accelerator Test Facility), Brookhaven for studying wakefields. Figure 2 is a schematic of a portion of the beam line, showing transverse radiation output by use of a 45° deflecting mirror. The vacuum window is made of Z axis cut crystal quartz for optimum transmission of the radiation over a wide range of wavelengths. A prior determination of the microwave spectrum of wakefield radiation using the radial probe, SMA, which permits one to determine the period of the wakefield, has been reported [6].

We now present a brief summary of an analysis for the fields set up within a structure of the type described. The theory has been thoroughly developed in recent years [7–

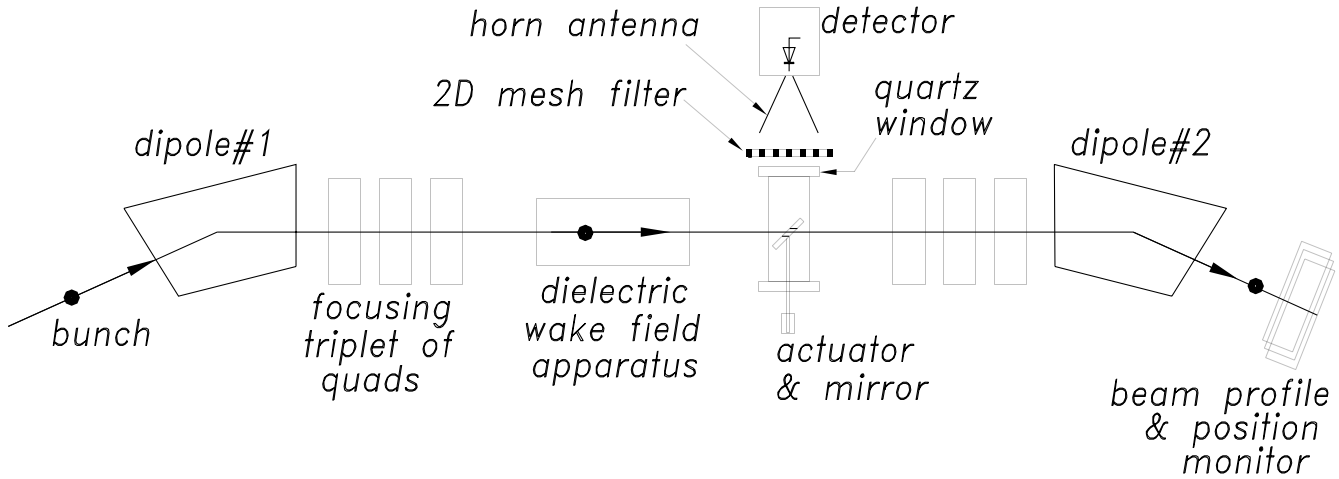

FIG. 2. Schematic of a portion of the beam line, showing transverse radiation output by use of a 45° deflecting mirror.

12]. In cylindrical geometry, orthonormal wave functions can be found for the fields which separate into TE and TM classes for axisymmetric excitations, and into hybrid modes with mixed polarization otherwise. With axisymmetric bunch distributions, only TM modes have an electric field (E_z) that is finite at the bunch location, and that consequently contributes to the radiation generated. Axisymmetric TE modes have vanishing electric fields on axis. Nonaxisymmetric modes that contribute to (unstable) transverse motions are excited by a bunch moving off axis [12]. Conditions can be found where all TM modes have phase velocities equal to the speed of the electrons ($v \cong c$), and so wakefields move in synchronism with the bunches. We neglect contributions from transition radiation localized near axial boundaries of the dielectric insert [13]. E_z-field component for the complete orthonormal TM mode set along an infinitely long waveguide can be written in the form

$$E_z(r, z, t) = \sum_m E_m \exp(-i\omega_m z_o/v) f_m(r)/\alpha_m, \quad (1)$$

where α_m is a normalizing constant, $z_o = z - vt$, and f_m is an expression involving Bessel functions which describes the radial dependence of the solution [10]. Wave numbers in the vacuum channel and in the dielectric are related by

$$k_{1m}^2 + \omega_m^2/v^2 = \omega_m^2/c^2, \quad (2a)$$

$$k_{2m}^2 + \omega_m^2/v^2 = \omega_m^2/\kappa c^2, \quad (2b)$$

where the evanescent transverse wave number in the vacuum is k_{1m}, the real transverse wave number in the dielectric is k_{2m}. Thus $k_{1m} = \omega_m/c\beta\gamma = k_{2m}\gamma_\kappa/\gamma$, where $\gamma_\kappa = (\kappa\beta^2 - 1)^{-1/2}$. The dispersion relation can be obtained [14], from which it is found that in the limit of high dielectric constant $\kappa \gg 1$, there is a nearly periodic spacing of eigenfrequencies where, for all but a few lowest modes, the mode separation is $\Delta\omega = \omega_{m+1} - \omega_m \approx \pi\beta c(R - A)^{-1}(\kappa\beta^2 - 1)^{-1/2}$. The wakefield is accordingly more strongly peaked and more nearly periodic in z_o as the eigenfrequencies become more nearly periodic and constructive phase interference between modes can occur. This constructive mode interference causes the wakefields to be localized at periodic intervals behind a moving bunch; the shorter the bunch, the greater the number of modes excited, and the more sharply peaked are these localized fields.

To find wakefields induced by an electron bunch, one expands in orthonormal modes the solution of the inhomogeneous wave equation and constructs a Green's function. For instance, for a bunch containing N_b electrons distributed along a finite rms length

$$\Delta z = 2\sqrt{\langle z^2\rangle - \langle z\rangle^2} \quad (3)$$

in a Gaussian function (symmetrical distribution), one finds

$$E_z(r, z, t) = -E_o \sum_m [f_m(r)/\alpha_m] \cos(\omega_m z_o/v) \times \exp(-\omega_m^2 \Delta z^2/8v^2). \quad (4)$$

Here, $E_o = -eN_b/2\pi\varepsilon_o A^2$, and the results are valid only behind the bunch ($z_o < 0$), following the dictates of causality; in front of the bunch $E_z = 0$. Note that only the radius of the hole A, and the bunch charge $-eN_b$ determine the total magnitude of the wakefield, while the bunch width Δz determines the distribution of amplitudes among the spectrum of normal modes. The energy loss dW/dz and total radiated power scale as ${N_b}^2$. Everywhere behind the Gaussian bunch

$$dW/dz = \frac{N_b^2 e^2}{4\pi\varepsilon_0 A^2} \sum_m [\exp(-\omega_m^2 \Delta z^2/8v^2)]^2/\alpha_m. \quad (5)$$

Numerical solutions for the wakefields are shown in the figures below for examples which might be typical in a diagnostic application: the parameters are from experiments carried out at ATF-Brookhaven, which uses 50 MeV electron bunches (asymmetrical distribution) obtained from an rf linac. The dimensions of the dielectric insert are chosen to provide a fundamental wakefield period in this device of 21 cm, which is twice the linac rf wavelength. This choice has to do with the method used for generating bunches, which uses time-delayed optical pulses incident upon the ATF rf photocathode gun.

An example of the power spectrum which we predict to be emitted from a typical well-focused bunch obtained at ATF, Brookhaven, is shown in Fig. 3. Radiation spectra from a Gaussian charge distribution having different rms lengths are shown. Most of the power is contained in the mm-wave portion of the spectrum. A high frequency ''cutoff'' limit can be identified by fitting a straight line to the descending slope of the high frequency radiation spectrum, projecting it onto the horizontal axis. Millimeter diagnostic spectroscopy can be carried out up to ~500 GHz, thus the technique can be adapted to bunches having length in the sub-psec region. However, we have found that the choice of axial charge distribution is not important, providing each distribution is characterized by the same bunch rms length. In Fig. 3(b), we show a spectrum generated by three different bunch shapes: a Gaussian, a triangular, and a rectangular charge distribution along the bunch-length axis. For each example, the same rms length is chosen for the bunch. The result is quite interesting, as it shows that as long as the bunch rms length is used for comparison, the spectrum generated is almost the same. This establishes the utility of the diagnostic, since the details of the bunch charge distribution do not significantly affect the measurement of the key parameter: namely, the bunch rms length. The physical reason for this result is that coherent bunch radiation requires generation of wavelengths which are longer than the bunch. These wavelengths cannot yield

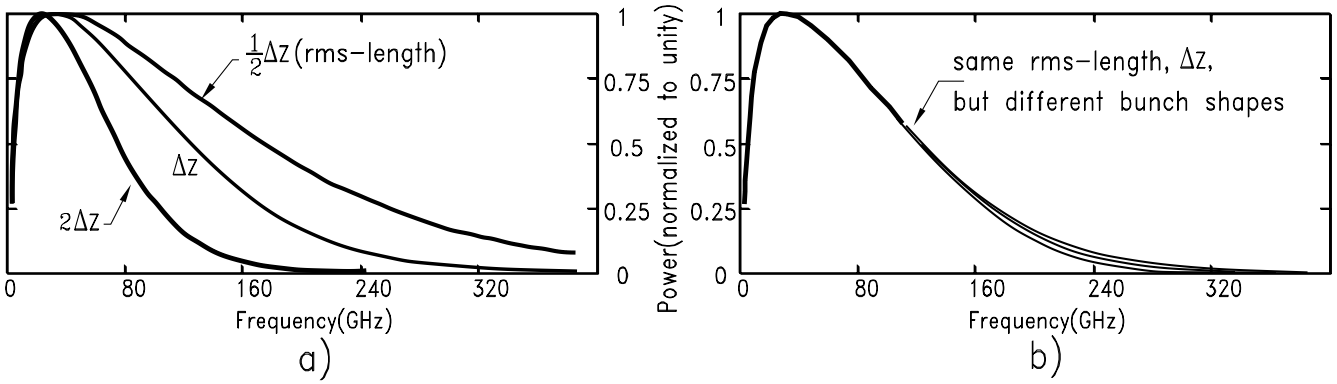

FIG. 3. Power spectrum that we predict to be emitted from a typical well-focused bunch obtained at ATF-BNL. (a) Radiation from a Gaussian charge distribution having different rms length (here $\Delta z = 1.8$ psec, and for the sake of convenience, we measure the rms length in units of time, i.e., $\Delta z = 1.8$ psec corresponds to $c \times 1.8$ psec ≈ 540 μm); (b) spectrum generated by three different bunch shapes: a Gaussian, an asymmetrical triangular (tail/head $= 4/1$), and a rectangular charge distribution along the bunch-length axis.

information about the fine-scale charge or current variation within the bunch. Accordingly, one finds, examining Fig. 3(b) , that whatever sensitivity to the bunch charge profile is revealed only at the shortest wavelengths.

For a nonaxisymmetric bunch charge distribution, hybrid modes will be excited in addition to the set of TM modes as described above [12]. However, the general dependence of the spectrum upon bunch length involves the same features described here for the TM modes.

III. EXPERIMENT

This experiment has been run on beam line #2 at ATF. The radiation is deflected from the bunch by a reflector (mirror) with a slot (12.7×3.57 mm wide) to permit the bunch to pass, and passes through a Z-cut quartz vacuum window into the experimental area [Fig. 4]. The mirror reflecting surface is tilted by 45° to the bunch trajectory.

The radiation is in the form of a single pulse for each bunch having a duration of roughly 1.7 nsec and kW level (Fig. 5).

We analyze the spectrum using a set of 5 cm $\times$ 5 cm calibrated metal mesh filters mounted onto a turntable structure which is driven by an external motor so that meshes with different filter functions can be rotated into the beam of millimeter radiation emerging from the window, using a remote control. The range of filtered frequencies is from 55 to 120 GHz. The detector is a Schottky-barrier diode which has been calibrated, along with the meshes, by the manufacturer Virginia Diodes, Inc. Attenuation is provided by a pad of white notepaper, so that the detector operates in its linear regime. We confirmed experimentally that at the chosen attenuation the transition radiation generated by the mirror slot is of negligible contribution to the detector signal. This was done via a comparison of the signal strengths with and without the dielectric wakefield apparatus. To make the comparison valid, we ensured that the electron beam was the same in each case by removing the dielectric section and observing the bunch profile, which was found to be the same both with and without the dielectric apparatus.

In order to validate the diagnostic method it is necessary to measure the bunch rms length using independent means at ATF. To measure the bunch rms length (as well as the bunch longitudinal distribution), a variable phase shift is introduced for the second rf linac section. A particle located at the head of the bunch thereby gains a different energy than one located at the tail. Thus the bunch profile along the time axis is mapped onto an energy axis. After passing through a dipole, the bunch trajectory experiences a transverse shift for every energy shift. Using a slit followed by a monitor, one can scan the charge profile of the bunch as the linac phase is varied (about 0.973 psec/degree). Other diagnostic information, such as bunch charge or energy lost from the bunches, is obtained routinely from the permanent ATF facility hardware available to all users. The measurements being done here are part of a larger program involving the study of the superposition of wakefields from multibunch trains.

The experiment has been successfully run, having started first with the development of a detailed plan for aligning the equipment and transporting up to three bunches through the hardware. The rms diameter of the bunch at the entry and exit to the dielectric element is in the range of 250–300 μm, and thus it is well removed from the walls of the dielectric channel. Thus far, two bunches, following each other separated by 10.5, 21, or 31.5 cm, have been transported through the hardware, suffering negligible particle losses; this disposes of any reservations having to do with the charging up of the channel walls and the potentially harmful effects that might thereby result. The transport system is achromatic, accommodating an input bunch energy variation of up to 1 MeV without affecting the bunch transport. Multiple bunches are used for studies of the superposition of wakefields, but in the

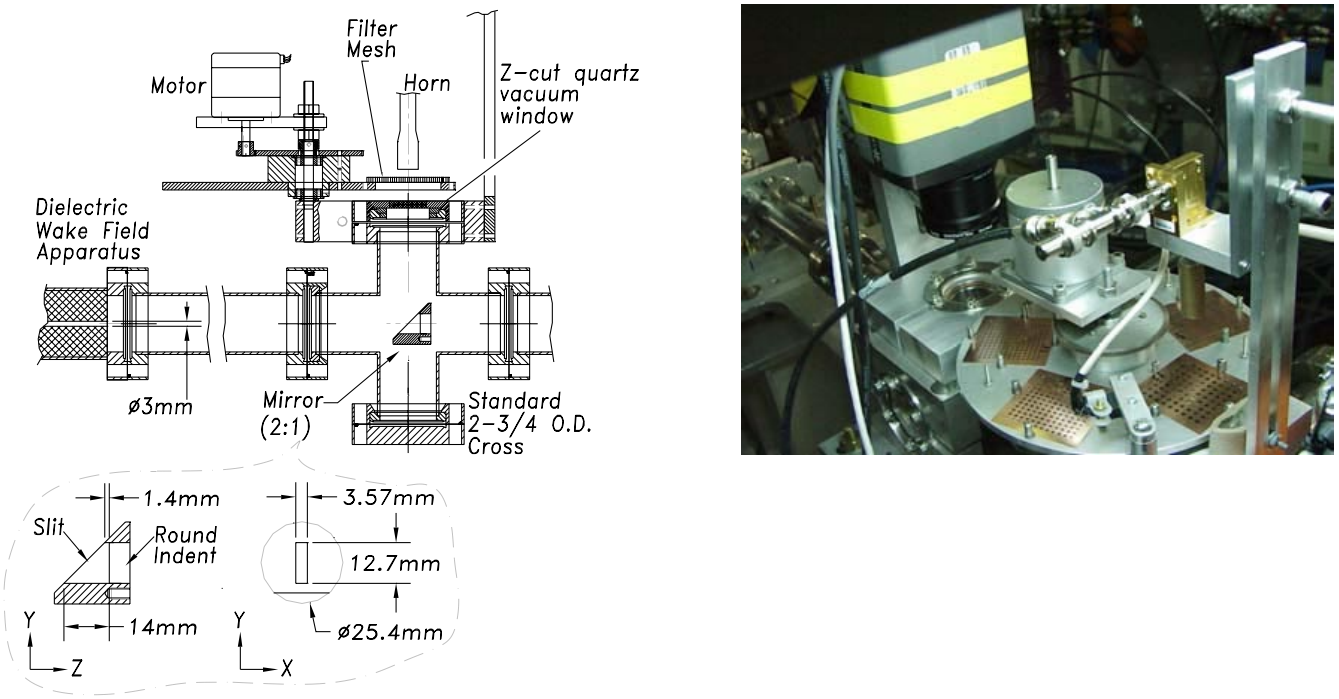

FIG. 4. (Color) Drawing of a portion of the beam line (left), showing transverse radiation output using a 45° deflecting mirror, and a picture of the apparatus, showing the detector, horn antenna, and rotational table equipped with 2D-mesh filters (transverse radiation output is below the table).

spectrum study which follows, we use only one bunch to generate the radiation.

Figure 6 shows how the filters break the spectrum of wakefield radiation into five channels. The solid line is the theoretical emitted spectrum from a single bunch having the rms length of 4.2 psec and charge 310 pC, being an envelope of the closely spaced TM_{0m} modes (separation $\approx$ 2.86 GHz). The metal mesh filters have transmission curves $T(\omega_m, \omega_F)$ centered at frequencies $\omega_F/2\pi = 54$, 68, 83, 98, and 117 GHz. It is seen that the half-transmission width of the filters is $\sim$10 GHz, thus $\sim$4 TM modes are accepted by each filter. Figure 7 shows the theoretical transmission characteristic and the measured transmission characteristic as done by the vendor, Virginia Diodes, Inc., for the filter with 117 GHz central frequency.

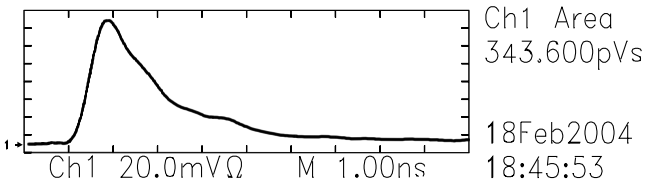

FIG. 5. Example of the detector response (after the 68 GHz filter, and the bunch with $\Delta z \approx 5.6$ psec); the horizontal scale is 1 ns/div; the vertical scale is 20 mV/div.

The detector responds to the square of the electric field, thus its signal $V(\omega_F, Q, \Delta z, t)$ depends on the sum of the squares of the amplitude coefficients of the TM modes (t is time). The integrated detector response $D(\omega_F, Q, \Delta z) \equiv \int V(\omega_F, Q, \Delta z, t)dt$ would be proportional to the area under the transmission curve of a particular mesh, i.e., $\sum_m T(\omega_m, \omega_F)P(\omega_m, \Delta z, Q)$, where $P(\omega_m, \Delta z, Q)$ is the power radiated by a single bunch with the charge Q and

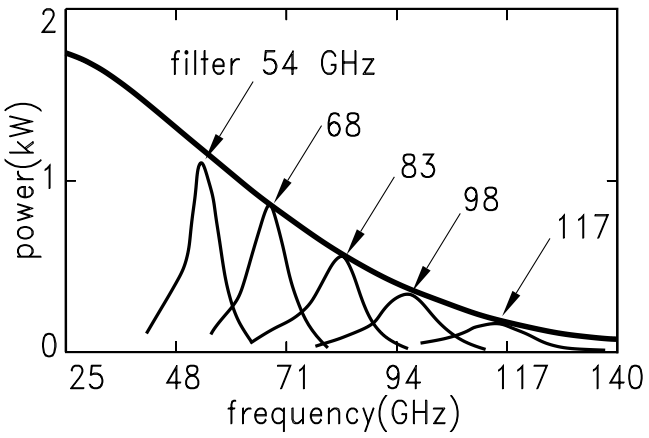

FIG. 6. Filters break the spectrum of wakefield radiation into five channels. The solid line is the theoretical emitted spectrum from a single bunch having rms length of 4.2 psec and charge 310 pC.

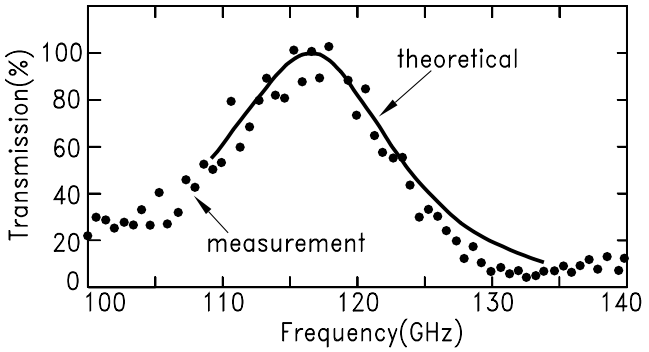

FIG. 7. An example of the transmission characteristic for the filter with 117 GHz central frequency. The theoretical transmission curve, and the experimental points are computed and measured by the vendor.

rms length Δz into the TM_{0m} eigenmode. Referring to Fig. 3, we point out that $P(\omega_m, \Delta z, Q)$, and consequently the integrated detector response $D(\omega_F, Q, \Delta z)$ is determined by and sensitive to the bunch rms length, whereas the details of the longitudinal distribution are not important.

We may, of course, observe the entire millimeter spectrum at frequencies centered on $\omega_F/2\pi = 54$, 68, 83, 98, and 117 GHz, as provided by the different meshes. With the narrow bandwidth filter the detector integrated response will be (see Fig. 8)

$$D = R(\omega_F)H(\omega_F)\sum_m T(\omega_m, \omega_F)P(\omega_m, \Delta z, Q). \quad (6)$$

The detector responsivity $R(\omega_F)$, which includes the contribution from the horn it is connected to and negligibly varies within the bandwidth of a filter, depends on wavelength. This has been measured by the vendor. However, there may be other wavelength-dependent transmission effects [characterized by the hardware responsivity $H(\omega_F)$] associated with the radiation emerging from the dielectric, transmitted by the overmoded beam transport pipe, and reflected by the mirror (Fig. 8).

Fortunately, if we form the ratio $R_{cp} \equiv D_1/D_2$ of detector integrated responses at each channel (fixed wavelength ω_F) for two different bunch lengths Δz_1 and Δz_2, then the wavelength dependence of the hardware response $H(\omega_F)$ will cancel at each frequency, and the ratio R_{cp} will be determined only by rms lengths Δz_1 and Δz_2, and bunch charges Q_1 and Q_2. In Fig. 9 we show how the ratio varies with frequency for a particular choice of bunch lengths $\Delta z_1 = 3.9$ and $\Delta z_2 = 1.7$ psec, and charges $Q_1 = Q_2 =$ 100 pC. The two curves (dotted and solid) nearly overlaying each other describe two ways of forming that ratio: using the total energy transmitted by the filter (*ratio of sums*)

$$R_{cp}(\omega_F, Q_1, Q_2, \Delta z_1, \Delta z_2) = \frac{\sum_m T(\omega_m, \omega_F)P(\omega_m, \Delta z_1, Q_1)}{\sum_m T(\omega_m, \omega_F)P(\omega_m, \Delta z_2, Q_2)} \quad (7)$$

or using the maximum of the filtered transmitted power (*ratio of maximums*)

$$R_{cp}(\omega_F, Q_1, Q_2, \Delta z_1, \Delta z_2) = \frac{\max_{1\le m<\infty} [T(\omega_m, \omega_F)P(\omega_m, \Delta z_1, Q_1)]}{\max_{1\le m<\infty} [T(\omega_m, \omega_F)P(\omega_m, \Delta z_2, Q_2)]}, \quad (8)$$

where we use the symbol $\max_{1\le m<\infty}$ to indicate that we search the maximum over all excited modes. The fact that either way of forming R_{cp} gives nearly the same result is confirmed for the range of rms lengths: 0.1 psec $\le \Delta z_1$,

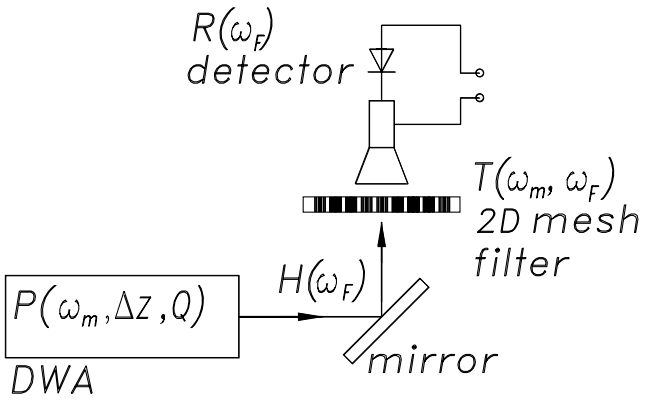

FIG. 8. Schematics of power transmission from the DWA to the detector through a narrow bandwidth filter, and the overmoded beam transport pipe.

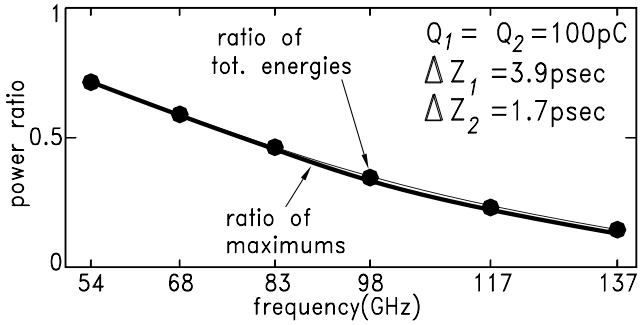

FIG. 9. Ratio of power emitted into each channel (fixed wavelength) for two different bunch lengths (3.9 and 1.7 psec) and charges (166 and 105 pC). The two curves nearly overlaying each other describe two ways of forming that ratio: using the total energy transmitted by the filter see Eq. (7), or using the maximum of the filtered transmitted power see Eq. (8).

$\Delta z_2 \leq 10$ psec. This range is sufficiently large for every rms length encountered in the experiment to fall into it.

With the functional form of R_{cp} known [Eq. (7)], we proceed to validate the bunch rms length diagnostic measurement as follows:

(i) First, one assumes that the rms length Δz_1 and charge Q_1 of a so-called reference bunch is known. Then, for every filter one measures the detector integrated response $D_1(\omega_F) = \int V_1(\omega_F, Q_1, \Delta z_1, t)dt$ (e.g., the area under the curve in Fig. 5).

(ii) Next, for a bunch whose rms length Δz_2 is unknown, one measures the charge Q_2 and, again for each filter, the detector integrated response $D_2(\omega_F) = \int V_2(\omega_F, Q_2, \Delta z_2, t)dt$.

(iii) Then, one forms a ratio R_{cp} according with Eq. (7), and compares it with D_1/D_2. One expects that a relationship

$$\frac{D_1(\omega_F)}{D_2(\omega_F)} \approx R_{cp}(\omega_F, Q_1, Q_2, \Delta z_1, \Delta z_2) \qquad (9)$$

must be satisfied for each filter.

Thus, one has several equations in which only one parameter is unknown, namely, the rms length Δz_2. Solving them, one finds the rms length Δz_2. As a matter of fact, one also may omit measuring the charge Q_2 because there are several filters, and even with two unknown parameters Q_2 and Δz_2 one still has an overdetermined system of equations which should allow finding both the charge Q_2, and unknown rms length Δz_2.

Regarding determining the reference parameters Q_1 and Δz_1 one notices that implementation of many narrow bandwidth filters (about 10 or more) results in a set of equations [each identical to Eq. (9)] that depends only on four parameters Q_1, Q_2, and Δz_1 and Δz_2. This system is still overdetermined, and always allows finding Q_1 and Δz_1. Consequently one may obtain all the required reference parameters: namely, the set of values $D_1(\omega_F)$, and the reference charge Q_1 and reference rms length Δz_1 without independent measurement. Thus, the proposed bunch diagnostic is self-sufficient since it does not require any other independent techniques to establish reference parameters.

A waveguide (or other similar structure) might be used to divide the power collected by the horn into several channels each followed by a narrow bandwidth filter with its own detector. Then all signals $D(\omega_F)$ are measured at the same moment of time, and the bunch diagnostic (i)–(iii) will provide shot-by-shot monitoring of the bunch charge and rms length.

One can appreciate that the approach using signal ratios, in addition to being accurate, is also simple, in that a few fixed-frequency channels can be used, and considerable expense can be avoided since no absolute measurement of the transmission function of these components is necessary. Needless to say, ease of use and accuracy are important considerations for choosing a bunch-length diagnostic.

To establish the feasibility of this technique, Eq. (9) must be verified experimentally using bunches of known charge and rms length. The experiment at ATF has generated data which permit the measurement of the length of charge bunches provided by the rf linac (50 MeV), and enough data have already been gathered to verify Eq. (9). The left-hand side of Eq. (9) is directly measured as the ratio of detector signals, D_1/D_2, and the right-hand side, R_{cp}, is computed after one has measured the charges and rms lengths (to change rms length one adjusts the delay between rf (2856 MHz) and the laser pulse (~ 7 psec FWHM) incident to the gun photocathode). One expects that within the measurement accuracy one should always have $D_1/D_2 \approx R_{cp}$.

In Fig. 10 we show data acquired for two cases: a 5.6 psec long bunch having charge 430 pC, and a 4.2 psec long bunch having charge 310 pC. The solid black line is the computed R_{cp} for these two different bunches. The "error bars" on this *line* represent the possible range of variation (two-sigma at each point) of R_{cp} due to errors in measurement of bunch charge ($\pm$ 30 pC by a Faraday cup) and bunch rms length ($\pm$ 0.2 psec). The dots represent the measured ratio D_1/D_2 at each filter frequency for the two types of bunch. It is found that the measured D_1/D_2 ratio and the computed R_{cp} are the same within the accuracy range.

There is very little variation of signal behavior from one shot to another, which suggests that charge measurements performed by a Faraday cup are noisier than the actual

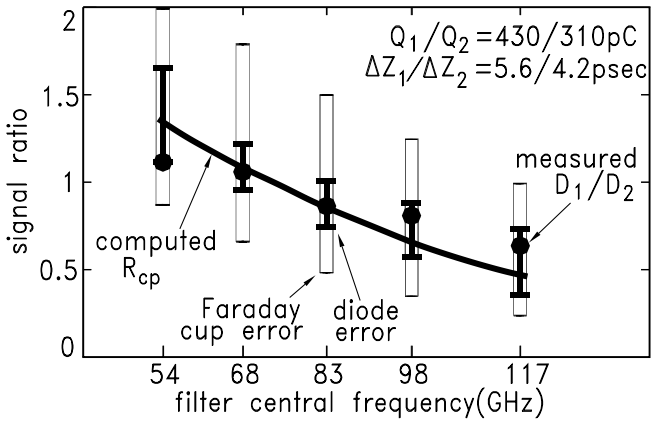

FIG. 10. Comparison of the computed R_{cp} with the measured D_1/D_2 for each channel (fixed wavelength) for two different bunch lengths (5.6 and 4.2 psec) and charges (430 and 310 pC). The solid black line is the computed R_{cp} after one has measured bunch charges, and rms lengths by an independent technique. The dots represent the measured D_1/D_2. The variation in charge from one shot to another measured by a Faraday cup results in large vertical error bars (hollow bars). The variation in charge derived from the signal variation of the detector, on contrary, results in smaller error bars (diode error) (see explanation in the text).

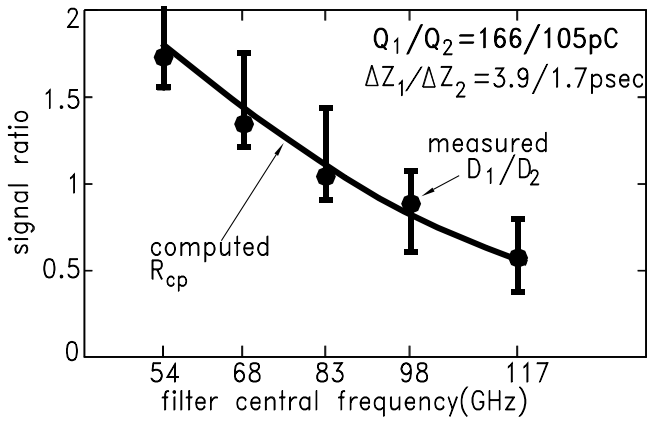

FIG. 11. Comparison of the computed R_{cp} with the measured D_1/D_2 for each channel (fixed wavelength) for two different bunch lengths (3.9 and 1.7 psec) and charges (166 and 105 pC). The solid black line is the computed R_{cp} after one has measured bunch charges, and rms lengths by an independent technique. The dots represent the measured D_1/D_2. The variation in charge from one shot to another is measured by calculating the charge variation from the signal variation of the detector.

charge variations. Based on the detector signal one would conclude that the variation in charge is much smaller; thus, the actual ''error bars'' are smaller (see ''diode error'' in Fig. 10). Figure 11 shows data acquired for two cases: a 3.9 psec long bunch having charge 166 pC, and a 1.7 psec long bunch having charge 105 pC. The solid black line is the computed R_{cp} for these two different bunches. The error bars on this line represent the possible range of variation (two-sigma at each point) of R_{cp} due to errors in measurement of bunch charge ($\pm$ 3 pC by calculating the charge variations through signal variations on the detector) and bunch rms length ($\pm$ 0.2 psec). This considerably improves the interpretation of the data in terms of our model.

Figure 12 shows more examples. Again, the error bars represent the possible range of variation (two-sigma at each point) of R_{cp} due to errors in measurement of bunch charge (about $\pm$3 pC by calculating the charge variations through signal variations on the detector) and bunch rms length (about $\pm$0.2 psec).

All experimental data (we performed measurements at $\Delta z \approx 5.6$, 4.2, 3.9, 3.0, 1.9, and 1.7 psec) behave in full agreement with the expectation. Namely, it is found that within the measurement accuracy Eq. (9) is satisfied for each filter central frequency.

IV. SUMMARY AND DISCUSSION

With Eq. (9) established one can use the proposed technique to measure the bunch rms length (and the bunch charge), by measuring the high-frequency spectrum of wakefield radiation which is caused by the passage of a relativistic electron bunch through a channel surrounded by a dielectric. The proposed technique (a) is nondestructive, (b) is routine to calibrate (it does not require any other independent technique to perform calibration), and (c) can be a single-shot technique.

The accuracy $\delta\Delta z/\Delta z$ of measurement of rms length Δz is found to be

$$\delta\Delta z/\Delta z = (C_{\Delta Z}/\Delta z^2) \times (\Delta D/2D), \qquad (10)$$

where $\Delta D = 2\sqrt{\overline{D^2} - D^2}$ is the fluctuation (double-sigma) of the detector signal. The coefficient $C_{\Delta Z}$ is determined by the structure parameters and the filter set. For the experiment at ATF with the range of filtered frequencies to 120 GHz, $C_{\Delta Z} \approx 13.8$ psec^2. With

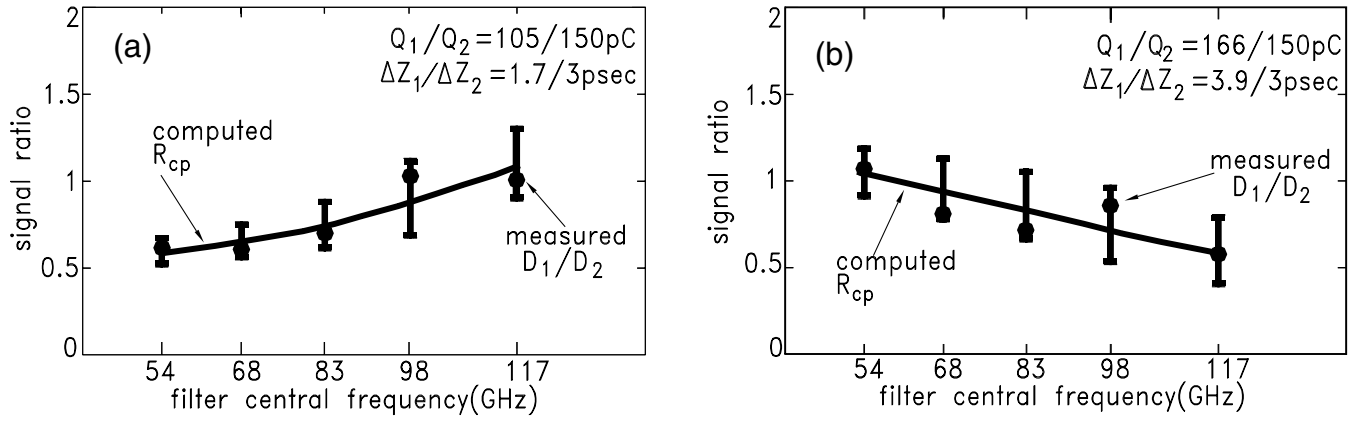

FIG. 12. (a) Comparison of the computed R_{cp} with the measured D_1/D_2 for each channel (fixed wavelength) for two different bunch lengths (3.9 and 3.0 psec) and charges (166 and 150 pC). The variation in charge from one shot to another is measured by calculating the charge variations from the signal variation of the detector. (b) Comparison of the computed R_{cp} with the measured D_1/D_2 for each channel (fixed wavelength) for two different bunch lengths (1.7 and 3.0 psec) and charges (105 and 150 pC). The variation in charge from one shot to another is measured by calculating the charge variations from the signal variation of the detector.

$\Delta D/2D \approx 1.5\%$, one may determine the rms length $\Delta z \approx$ 3–4 psec with an accuracy $\approx 1.5\%$.

The minimum rms length one can resolve with this technique is

$$\Delta z_{\mathrm{MIN}} = \sqrt{C_{\Delta Z} \times (\Delta D/2D)}. \tag{11}$$

For the ATF experimental setup and $\Delta D/2D \approx 1.5\%$, one may expect to resolve the rms length $\Delta z \geq 450$ fsec. Using the same dielectric-lined structure but changing to the range of filtered frequencies up to 300 GHz, one reduces $C_{\Delta Z} \approx 2.4$ psec^2. With $\Delta D/2D \approx 1.5\%$, one could resolve the rms length $\Delta z \geq 190$ fsec.

Measurement of the millimeter-wave spectrum will determine the bunch rms length in the *psec* range. With ever increasing interest within the accelerator community in new bunch-length monitors for bunches having sub-mm dimensions one also could consider the extension of this technique into the fsec range. The use of a microstructure configured as a set of tall planar dielectric slabs, 2 mm in height, 3.65 μm in width, separated by a vacuum channel having width of 10 mcm through which a 1 μm tall "planar slab" charge bunch moves a short distance is being considered [5,15]. A suitable dielectric may be ZnSe, dielectric constant = 5.76 in the far infrared. A multimode wakefield is set up by the moving bunch, having period $\sim$33 μm. The spectrum of modes extends to the region $\sim$2–3 μm; these modes are excited coherently by bunches with length $\sim$1 μm or longer, which might be obtained in laser accelerators (e.g., CO_2 laser driven, where the bunches are single, or spaced by the laser period of 10.6 μm). Thus, a study of wakefield radiation in the infrared which is emitted by such a small structure might be useful in determining the lengths of bunches $\sim$3 fsec or longer. The suitability of this approach requires further study.

So far we have discussed the spectrum emitted by just one bunch; however, we may comment on the case when several bunches are actually provided. If one superimposes the radiation fields of several equally spaced bunches, then the shape of the spectrum depends markedly upon the ratio of the wakefield period to the bunch spacing.

If this ratio is an even number, then the high frequency spectrum (where the modes are evenly spaced) is severely attenuated; if this ratio is an odd number, then the power spectrum envelope resembles that of a single bunch, albeit enhanced in magnitude, with certain TM modes deleted. If the ratio is neither even nor odd, the spectrum is so complicated that it is likely to be useless for bunch-length diagnostic purposes. To illustrate this odd/even behavior (Fig. 13), we have taken the parameters of the ATF wakefield apparatus, where the wakefield period is 21 cm, to compute the spectrum for a train of bunches with spacing 1/2, 1/3, and 1/4 the wakefield period. The example in the top plot demonstrates that if the wakefield apparatus is configured so that its wakefield period is an odd multiple of the bunch spacing, the spectrum will allow very straightforward interpretation because its envelope (i.e., the line connecting the points with the maximum amplitudes) will be the same as the envelope of the spectrum of a single bunch; the wakefield period can be adjusted by correct choice of the dielectric thickness.

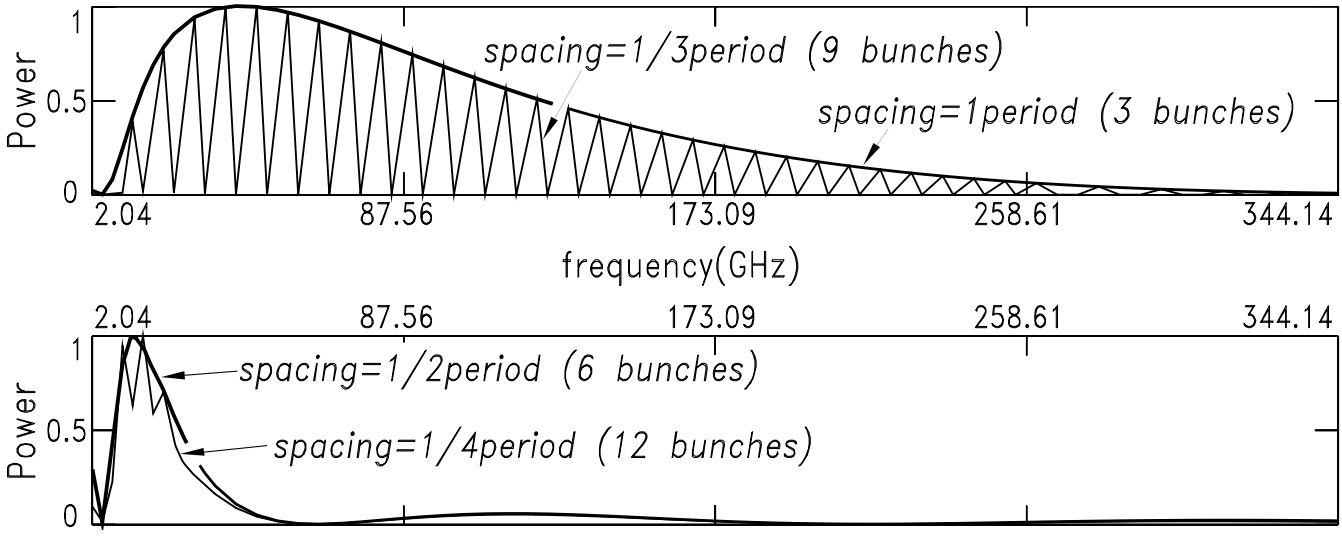

FIG. 13. Normalized spectrum for a train of bunches with spacing 1, 1/2, 1/3, and 1/4 the wakefield period, normalized to the same maximum value. The shape of the spectrum depends upon the ratio of the wakefield period to the bunch spacing. If this ratio is an odd (top) or even (bottom) number, one can interpret the high frequency spectrum to obtain the rms length. If the ratio is neither odd nor even, the spectrum is so complicated that is likely to be useless for diagnostic purposes. (Here, the train has 3 identical bunches when the spacing is 1 wakefield period, 6 identical bunches when the spacing is 1/2 of the wakefield period, 9 identical bunches when the spacing is 1/3 of the wakefield period, and 12 identical bunches when the spacing is 1/4 of the wakefield period.)

ACKNOWLEDGMENTS

The authors acknowledge the help received from the ATF staff: I. Ben-Zvi, M. Babzien, T. Watanabe, F. Zhou, and V. Yakimenko. This work was supported by the Department of Energy High Energy Physics Division.

[1] See, e.g., J. C. Swartz, B. D. Guenther, F. C. De Lucia, W. Guo, C. R. Jones, H. Kosai, and J. M. Dutta, Phys. Rev. E **52**, 5416 (1995), and references therein.

[2] See, e.g., R. Miller, SLAC-TN-63-065, 1963.

[3] S. V. Shchelkunov, T. C. Marshall, J. L. Hirshfield, and M. A. LaPointe, in *Advanced Accelerator Concepts: Eleventh Advanced Accelerator Concepts Workshop*, edited by V. Yakimenko, AIP Conf. Proc. No. 737 (AIP, New York, 2004), p. 421.

[4] J. Mollá, R. Moreno, and A. Ibarra, J. Appl. Phys. **80**, 1028 (1996), and references therein.

[5] C. Wang, J. L. Hirshfield, J-M. Fang, and T. C. Marshall, Phys. Rev. ST Accel. Beams **7**, 051301 (2004).

[6] J-M. Fang, T. C. Marshall, J. L. Hirshfield, M. A. LaPointe, T-B. Zhang, and X. J. Wang, in *Proceedings of the 1999 Particle Accelerator Conference*, edited by Luccio and MacKay (IEEE, New York, 1999), Vol. 5, p. 3627.

[7] K-Y. Ng, Phys. Rev. D **42**, 1819 (1990).

[8] M. Rosing and W. Gai, Phys. Rev. D **42**, 1829 (1990).

[9] W. Gai, P. Schoessow, B. Cole, R. Konecny, J. Rosenzweig, and J. Simpson, Phys. Rev. Lett. **61**, 2756 (1988).

[10] T-B. Zhang, J. L. Hirshfield, T. C. Marshall, and B. Hafezi, Phys. Rev. E **56**, 4647 (1997).

[11] J. G. Power, W. Gai, and Paul Schoessow, Phys. Rev. E **60**, 6061 (1999).

[12] S. Y. Park and J. L. Hirshfield, Phys. Rev. E **62**, 1266 (2000).

[13] I. N. Onishchenko, D. Yu. Sidorenko, and G. V. Sotnikov, Phys. Rev. E **65**, 066501 (2002).

[14] C. T. M. Chang and J. W. Dawson, J. Appl. Phys. **41**, 4493 (1970).

[15] T. C. Marshall, C. Wang, and J. L. Hirshfield, Phys. Rev. ST Accel. Beams **4**, 121301 (2001).